Ξ hypernuclei $^{15}_{\Xi}$C and $^{12}_{\Xi}$Be, and the Ξ*N* two-body interaction

Yusuke Tanimura,[1,2] Hiroyuki Sagawa,[3,4] Ting-Ting Sun,[5] and Emiko Hiyama[1,4]

[1]*Department of Physics, Tohoku University, Sendai 980-8578, Japan*
[2]*Graduate Program on Physics for the Universe, Tohoku University, Sendai 980-8578, Japan*
[3]*Center for Mathematics and Physics, the Univeristy of Aizu, Aizu-Wakamatsu, Fukushima 965-8580, Japan*
[4]*RIKEN, Nishina Center, Wako, Saitama 351-0198, Japan*
[5]*School of Physics and Microelectronics, Zhengzhou University, Zhengzhou 450001, China*

(Received 8 February 2022; accepted 1 April 2022; published 25 April 2022)

We study the energy spectra of Ξ hypernuclei $^{15}_{\Xi}$C and $^{12}_{\Xi}$Be with a relativistic mean field (RMF) model with meson exchange Ξ*N* interactions. The RMF parameters are optimized to reproduce the average energy of KINKA and IRRAWADDY events for the ground state and also the average energy of KISO and IBUKI events for the excited state in $^{15}_{\Xi}$C. The potential depth of the average Ξ*N* mean field potential is found to be about −12 MeV in the nuclear matter limit. We further introduce the two-body *s*- and *p*-wave interactions between valence nucleons and Ξ particle. We found that the *s*-wave interaction deduced from the HAL lattice QCD results is rather weak to obtain the energy difference between IRRAWADDY and KINKA events. The *p*-wave interaction is added and fitted to reproduce the energy difference. The resulting interaction together with the *s*-wave one gives a reasonable energy simultaneously for IBUKI event as an excited Ξ_p state. The model is further applied to predict the energy spectrum of $^{12}_{\Xi}$Be.

DOI: 10.1103/PhysRevC.105.044324

I. INTRODUCTION

The study of interaction of the strangeness $S = -2$ sector is important in hypernuclear physics. To this end, so far several YY potential models such as that of the Njimegen group [1] and chiral effective field theory [2] have been proposed. However, due to the difficulty of performing hyperon-hyperon (Y-Y) scattering experiments, the proposed potentials have a large ambiguity depending on the models. Instead, as an alternative way to obtain information on the $S = -2$ sector, more pragmatic models were proposed to reproduce empirical data with less ambiguity. For such approaches, it is crucial to study structure of double strangeness hypernuclei such as double Λ hypernuclei and Ξ hypernuclei. Experimentally, some double Λ hypernuclei, $^{6}_{\Lambda\Lambda}$He (NAGARA event) [3,4], $^{10}_{\Lambda\Lambda}$Be (DEMACHI-YANAGI event) [4], and $^{11}_{\Lambda\Lambda}$Be (HIDA [4] and MIKAGE events [5]) have been observed by KEK-E373 and J-PARC-E07 experiments. In comparisons with the data and theoretical calculations, it was found that the $^1S_0$ of ΛΛ interaction is attractive, but much less attractive than that of the Λ*N* interaction. Further analysis of the J-PARC-E07 experiment is still in progress.

Regarding Ξ hypernuclei, the first evidence of a bound Ξ hypernucelus, $^{15}_{\Xi}$C (^{14}N+Ξ$^-$), was reported in 2015 by the KEK-E373 experiment, and is named KISO event [6]. At that time, there were two possible Ξ$^-$ binding energy interpretations from the analyses of the kinematic formation and decay modes, $\Xi^- + {}^{14}\mathrm{N} \to {}^{15}_{\Xi}\mathrm{C} \to {}^{10}_{\Lambda}\mathrm{Be} + {}^{5}_{\Lambda}\mathrm{He}$. One is $B_\Xi \equiv -E(^{14}\mathrm{N}) = 4.38 \pm 0.25$ MeV, assuming the ground state (g.s.) of $^{10}_{\Lambda}$Be after the decay from $^{15}_{\Xi}$C. The other is $B_\Xi = 1.11 \pm 0.25$ MeV, assuming the decay from the first excited state of $^{10}_{\Lambda}$Be. Afterwards, due to the revision of the observed binding energy of the $^{10}_{\Lambda}$Be, the B_Ξ of KISO event was updated accordingly to be 3.87 ± 0.21 MeV or 1.03 ± 0.18 MeV [7]. Thanks to the observation of KISO event, it was found that Ξ-nucleus interaction should be attractive, and it was necessary to interpret theoretically that KISO event is the observation of either ^{14}N(g.s.) + Ξ(1*s*) or ^{14}N(g.s.) + Ξ(1*p*). Motivated by the observed data in Ref. [6], some of the present authors (T.-T.S., H.S., and E. H.) studied the structure of $^{15}_{\Xi}$C using relativistic mean field (RMF) and Skyrme-Hartree-Fock (SHF) models, and interpreted KISO event as ^{14}N(g.s.) + Ξ(1*p*) [8]. Afterwards, ^{14}N(g.s.) + Ξ(1*p*) was observed as IBUKI event with the binding energy $B_\Xi = 1.27 \pm 0.21$ MeV [9]. Very recently, two new events ^{14}N(g.s.) + Ξ(1*s*) were reported by J-PARC-E07. One is called KINKA event and the other is called IRRAWADDY event [10]. The observed B_Ξ of the former is 8.00 ± 0.77 or 4.96 ± 0.77 MeV, and that of the latter is 6.27 ± 0.27 MeV. These observations could give a significant contribution to the information on *s*-wave Ξ*N* interaction. For the further study of Ξ*N* interaction, a search experiment for $^{12}_{\Xi}$Be at J-PARC by $^{12}C(K^-, K^+)$ reaction is planned.

Considering this situation, it is important to reproduce all of the observed events theoretically. We consider that KINKA and IRRAWADDY events are partners of the ground-state doublet and that IBUKI and KISO events are also partners of the excited-state doublet because there should exists $\sigma \cdot \sigma$ and $\tau \cdot \tau$ dependent terms in the Ξ*N* interaction, whereas the spin-orbit contribution is negligible for the ground state

doublet of ${}^{15}_{\Xi}$C. In this paper, we adopt the RMF model with the meson-exchange ΞN interactions, which were also employed in the previous paper [8]. In addition, in this paper, we introduce the $\sigma\cdot\sigma$ and $\tau\cdot\tau$ dependent two-body ΞN interactions for valence nucleons and Ξ particle. Parameters of the two-body ΞN interaction should be optimized so as to reproduce IRRAWADDY event and KISO event. Moreover, the ΞN interaction employed in ${}^{15}_{\Xi}$C is applied to the study of ${}^{12}_{\Xi}$Be. It is planned to produce ${}^{12}_{\Xi}$Be by (K^-, K^+) reaction using a ^{12}C target in the J-PARC-E70 experiment. To encourage the experiment, we predict energy spectra of this hypernucleus.

Since the core nuclei, ^{14}N and ^{11}B, have compact shell structure, it is hardly compressed by the addition of Ξ hyperon. Thus, the RMF approach is suited for the present work. In fact, in the previous paper [8], using RMF we accomplished interpreting KISO event as ^{14}N(g.s.) + $\Xi(1p)$. Thus it is highly expected that we can interpret IRRAWADDY event and predict low-lying level structure of ${}^{12}_{\Xi}$Be in a consistent manner.

This paper is organized as follows. Sec. II is devoted to the introduction of the model. Results of ${}^{15}_{\Xi}$C and ${}^{12}_{\Xi}$Be are presented in Sec. III. The average ΞN mean field potentials for various Ξ nuclei are also discussed in Sec. III. A summary is given in Sec. IV.

II. MODEL

A. Relativistic mean field model for Ξ hypernuclei

To describe the Ξ hypernucleus, we employ a meson-exchange model with nonlinear couplings for RMF theory [11]. The Lagrangian density is given by

$$\begin{aligned}\mathcal{L} &= \bar\psi_N(i\partial\!\!\!/ - m_N)\psi_N + \bar\psi_\Xi(i\partial\!\!\!/ - m_\Xi)\psi_\Xi \\ &+ \frac{1}{2}(\partial_\mu\sigma)(\partial^\mu\sigma) - \frac{1}{2}m_\sigma^2\sigma^2 - \frac{c_3}{3}\sigma^3 - \frac{c_4}{4}\sigma^4 \\ &- \frac{1}{4}G^{\mu\nu}G_{\mu\nu} + \frac{1}{2}m_\omega^2\omega^\mu\omega_\mu + \frac{d_4}{4}(\omega^\mu\omega_\mu)^2 \\ &- \frac{1}{4}\vec R^{\mu\nu}\cdot\vec R_{\mu\nu} + \frac{1}{2}m_\rho^2\vec\rho^\mu\cdot\vec\rho_\mu \\ &- \frac{1}{4}F^{\mu\nu}F_{\mu\nu} \\ &- \bar\psi_N\left(g_{\sigma N}\sigma + g_{\omega N}\omega\!\!\!/ + g_{\rho N}\vec\rho\!\!\!/\cdot\vec\tau_N + eA\!\!\!/\frac{1+\tau_{N,3}}{2}\right)\psi_N \\ &- \bar\psi_\Xi\left(g_{\sigma\Xi}\sigma + g_{\omega\Xi}\omega\!\!\!/ + g_{\rho\Xi}\vec\rho\!\!\!/\cdot\vec\tau_\Xi\right. \\ &\left. + \frac{f_{\omega\Xi}}{4m_\Xi}G_{\mu\nu}\sigma^{\mu\nu} + eA\!\!\!/\frac{-1+\tau_{\Xi,3}}{2}\right)\psi_\Xi, \end{aligned} \tag{1}$$

where ψ_N and ψ_Ξ are nucleon and Ξ hyperon fields, and $G^{\mu\nu} = \partial^\mu\omega^\nu - \partial^\nu\omega^\mu$, $\vec R^{\mu\nu} = \partial^\mu\vec\rho^\nu - \partial^\nu\vec\rho^\mu$, and $F^{\mu\nu} = \partial^\mu A^\nu - \partial^\nu A^\mu$ are the field tensors of the vector mesons ω and ρ and of the photon, respectively. $\vec\tau_N$ and $\vec\tau_\Xi$ are the Pauli matrices in the isospin space. Note that we follow the convention in which proton and Ξ^0 are regarded as the isospin-up states while neutron and Ξ^- isospin-down states. We adopt the PK1 parameter set [12] for the nucleon-meson couplings. The ρ-Ξ coupling constant is taken to be $g_{\rho\Xi} = g_{\rho N}$ as in Refs. [8,13]. The remaining coupling constants $g_{\sigma\Xi}$, $g_{\omega\Xi}$, and $f_{\omega\Xi}$ in the hyperon sector are fitted to experimental data (IRRAWADDY [10] and KINKA events; see Sec. III). The Ξ hyperon mass m_Ξ is taken to be 1321.7 MeV [14].

The model Lagrangian given above is solved within the mean field and the no-sea approximations. We impose time-reversal invariance and charge conservation of the mean field state, i.e., the time-odd or charged vector fields vanish. The only nonzero components are their timelike and neutral components, ω^0, ρ_3^0, and A^0, where the subscript 3 on the ρ meson field means the third component in the isospace.

The scalar-isoscalar density ρ_S, vector-isoscalar and -isovector densities j^0 and j_3^0 of nucleon are defined in terms of the single-particle wave functions of nucleon $\psi_k^{(N)}$ as

$$\rho_S(\boldsymbol{r}) = \sum_{k\in\mathrm{occ}}\bar\psi_k^{(N)}(\boldsymbol{r})\psi_k^{(N)}(\boldsymbol{r}), \tag{2}$$

$$j^0(\boldsymbol{r}) = \sum_{k\in\mathrm{occ}}\bar\psi_k^{(N)}(\boldsymbol{r})\gamma^0\psi_k^{(N)}(\boldsymbol{r}), \tag{3}$$

$$j_3^0(\boldsymbol{r}) = \sum_{k\in\mathrm{occ}}\bar\psi_k^{(N)}(\boldsymbol{r})\gamma^0\tau_3\psi_k^{(N)}(\boldsymbol{r}), \tag{4}$$

where k runs over the occupied nucleon states. The scalar, vector, and tensor densities of Ξ hyperon are defined in terms of the single-particle wave function of the Ξ hyperon $\psi_k^{(\Xi)}$ as

$$\rho_{S\Xi}(\boldsymbol{r}) = \bar\psi_k^{(\Xi)}(\boldsymbol{r})\psi_k^{(\Xi)}(\boldsymbol{r}), \tag{5}$$

$$j_\Xi^0(\boldsymbol{r}) = \bar\psi_k^{(\Xi)}(\boldsymbol{r})\gamma^0\psi_k^{(\Xi)}(\boldsymbol{r}), \tag{6}$$

$$j_{\Xi3}^0(\boldsymbol{r}) = \bar\psi_k^{(\Xi)}(\boldsymbol{r})\gamma^0\tau_3\psi_k^{(\Xi)}(\boldsymbol{r}), \tag{7}$$

$$\boldsymbol{V}_{T\Xi}(\boldsymbol{r}) = \bar\psi_k^{(\Xi)}(\boldsymbol{r})i\boldsymbol{\alpha}\psi_k^{(\Xi)}(\boldsymbol{r}), \tag{8}$$

where k here denotes the occupied Ξ hyperon state.

The equations of motion for the meson and electromagnetic fields read

$$\begin{aligned}\left(-\nabla^2 + m_\sigma^2\right)\sigma &= -g_{\sigma N}\rho_S - c_3\sigma^2 - c_4\sigma^3 \\ &\quad - g_{\sigma\Xi}\rho_{S\Xi},\end{aligned} \tag{9}$$

$$\begin{aligned}\left(-\nabla^2 + m_\omega^2\right)\omega^0 &= g_{\omega N}j^0 - d_4(\omega^0)^3 \\ &\quad + g_{\omega\Xi}j_\Xi^0 + \frac{f_{\omega\Xi}}{2m_\Xi}\nabla\cdot\boldsymbol{V}_{T\Xi},\end{aligned} \tag{10}$$

$$\left(-\nabla^2 + m_\rho^2\right)\rho_3^0 = g_{\rho N}j_3^0 + g_{\rho\Xi}j_{\Xi3}^0, \tag{11}$$

$$-\nabla^2 A^0 = e\left[\tfrac{1}{2}\left(j^0 + j_3^0\right) - \tfrac{1}{2}\left(j_\Xi^0 - j_{\Xi3}^0\right)\right]. \tag{12}$$

The Dirac equation for the nucleon single-particle wave function is given by

$$[-i\boldsymbol{\alpha}\cdot\nabla + V_N + \beta(m_N + S_N)]\psi_k^{(N)} = \epsilon_k\psi_k^{(N)}, \tag{13}$$

where

$$S_N = g_{\sigma N}\sigma, \tag{14}$$

$$V_N = g_{\omega N}\omega^0 + g_{\rho N}\rho_3^0\tau_{N,3} + eA^0\frac{1+\tau_{N,3}}{2}. \tag{15}$$

The Dirac equation for the single-particle wave function of the Ξ hyperon is given by

$$[-i\boldsymbol{\alpha}\cdot\boldsymbol{\nabla}+V_\Xi+\beta(m_\Xi+S_\Xi)+i\beta\boldsymbol{\alpha}\cdot\boldsymbol{T}_\Xi]\psi_k^{(\Xi)}=\epsilon_k\psi_k^{(\Xi)}, \tag{16}$$

where

$$S_\Xi = g_{\sigma\Xi}\sigma, \tag{17}$$

$$V_\Xi = g_{\omega\Xi}\omega^0 + g_{\rho\Xi}\rho_3^0\tau_{\Xi,3} + eA^0\frac{-1+\tau_{\Xi,3}}{2}, \tag{18}$$

$$\boldsymbol{T}_\Xi = \frac{f_{\omega\Xi}}{2m_\Xi}(-\boldsymbol{\nabla}\omega^0). \tag{19}$$

The set of equations (2)–(19) are solved self-consistently. In the numerical calculations, we further impose spherical symmetry, and the radial coordinate is discretized up to 40 fm with the step size of 0.1 fm. The spurious Ξ-Ξ interaction effect via the ρ meson is removed in the same way as in Ref. [13].

B. Residual interactions

We consider the spin-isospin-dependent residual interaction, which will be introduced in Sec. III. Once the residual interaction is given, its effect on the energy spectra of $^{15}_{\Xi}$C and $^{12}_{\Xi}$Be will be estimated by first-order perturbation theory. We construct the unperturbed states based on the RMF wave functions.

The ^{14}N subsystem of $^{15}_{\Xi}$C nucleus is described as the $p_{1/2}$ neutron and proton coupled to the total spin-parity $J_{np}^{\pi_{np}}=1^+$ and isospin $T_{np}=0$ on top of the inert ^{12}C core. The Ξ particle is then coupled to the nucleon pair to make the total quantum numbers $J^\pi T$, where J^π is the total spin-parity of the system, and $T=1/2$ in the case of $^{15}_{\Xi}$C. The energy shift due to the residual interaction $V_{N\Xi}$ is given as

$$\Delta E = \langle[[\nu 1p_{1/2}\,\pi 1p_{1/2}]^{1^+}\Xi nl_j]^{J^\pi} \times |V_{N\Xi}|[[\nu 1p_{1/2}\,\pi 1p_{1/2}]^{1^+}\Xi nl_j]^{J^\pi}\rangle, \tag{20}$$

where we take here the proton-neutron formalism, and the obvious isospin quantum number $T=1/2$ is implicit. nlj denote the radial quantum number and the orbital and total angular momenta of the Ξ particle, respectively.

The $^{12}_{\Xi}$Be nucleus is regarded as a particle-hole state, i.e., a $p_{3/2}$ nucleon hole and a $1s_{1/2}$ Ξ particle on top of the ^{12}C core, which are coupled to good angular momentum and isospin $J^\pi T$. In the case of $^{12}_{\Xi}$Be, the energy shift due to the residual interaction is given as

$$\Delta E = \left\langle\left[N1p_{3/2}^{-1}\,\Xi nl_j\right]^{J^\pi T}|V_{N\Xi}|\left[N1p_{3/2}^{-1}\,\Xi nl_j\right]^{J^\pi T}\right\rangle. \tag{21}$$

III. RESULTS

A. ΞN interaction and energy spectra of $^{15}_{\Xi}$C

We adjust the parameters, $g_{\sigma\Xi}$, $g_{\omega\Xi}$, and $f_{\omega\Xi}$ so as to reproduce the observed $B_\Xi=6.27\pm0.24$ MeV IRRAWADDY event for ^{14}N(g.s.) + Ξ($1s$) and the $B_\Xi=1.03\pm0.18$ MeV KISO event for ^{14}N(g.s.) + Ξ($1p$). It should be noted that we have other two observed data, IBUKI event, $B_\Xi=1.27\pm0.21$ MeV, and KINKA event, $B_\Xi=8.00\pm0.77$ MeV or 4.96 ± 0.77 MeV, which are expected to be ^{14}N(g.s.) + Ξ($1p$) and ^{14}N(g.s.) + Ξ($1s$), respectively. First, assuming KINKA event at $B_\Xi=4.96\pm0.77$ MeV and IRRAWADDY events are the ground-state spin doublet, and KISO and IBUKI events are a part of the excited-state multiplets, we fit the Ξ-ω Yukawa couplings $g_{\sigma\Xi}$ and $g_{\omega\Xi}$ as the parameter set (a) so that $B_{\Xi(1s)}$ is located between IRRAWADDY and KINKA, and spin-averaged $B_{\Xi(1p)}$ is close to KISO and IBUKI. Second, we take KINKA event at $B_\Xi=8.00$ MeV as the ground state and repeat the same procedure to determine the parameter set (b). In Ref. [15], KINKA event at $B_\Xi=8.00$ MeV was also adopted as the ground state for the parameter fitting of Skyrme-type Ξ-N interaction. Furthermore, we introduce Ξ-ω tensor coupling $f_{\omega\Xi}$ to produce the spin-orbit force of ΞN so that $B_{\Xi(1p_{3/2})}$ and $B_{\Xi(1p1/2)}$ are 0.86 and 0.72 MeV, respectively, for the set (a). The parameter set (a) thus determined leads to $B_{\Xi(1s)}=5.69$ MeV for the RMF ground-state binding energy. As for the parameter set (b), $B_{\Xi(1s)}=6.91$ MeV, $B_{\Xi(1p_{3/2})}=1.29$ MeV, and $B_{\Xi(1p1/2)}=1.13$ MeV. The resultant values of the coupling constants are tabulated in Table I. In view of the order of magnitude, our phenomenological values are consistent with the values with the naive quark counting and the quark model [16]. Note that $g_{\omega\Xi}/g_{\omega N}\approx0.5$ is close to the value adopted in the recent quark mean field model study [17].

Next, we study spin-isospin-dependent residual ΞN interactions. The s-wave interaction is defined by

$$V_{N\Xi} = \sum_{i\in\text{nucleons}}(v_\sigma\boldsymbol{\Sigma}_i\cdot\boldsymbol{\Sigma}_\Xi + v_\tau\vec{\tau}_i\cdot\vec{\tau}_\Xi + v_{\sigma\tau}\boldsymbol{\Sigma}_i\cdot\boldsymbol{\Sigma}_\Xi\vec{\tau}_i\cdot\vec{\tau}_\Xi)\delta(\boldsymbol{r}_i-\boldsymbol{r}_\Xi), \tag{22}$$

where $\boldsymbol{\Sigma}=\begin{pmatrix}\boldsymbol{\sigma} & 0\\ 0 & \boldsymbol{\sigma}\end{pmatrix}$ is the spin operator acting on a Dirac spinor. In this work, we use the information on a potential based on first-principle lattice QCD simulations, the HAL QCD ΞN potential (HAL potential) [18], in the following way: First we calculate volumes of HAL potential defined by

$$V_\beta = \int d^3r f_\beta(r)V_\beta^{\text{HAL}}(r), \tag{23}$$

where $\beta=0,\sigma,\tau,\sigma\tau$, and

$$f_\beta(r)=\frac{1}{1+\exp[-(r-R_\beta)/d]}. \tag{24}$$

Here, we take $d=0.1$ fm and $R_\beta=(0.234, 0.816, 0.548, 0.684)$ fm for the spin-isospin channels $(2S+1, 2T+1)=(11, 31, 13, 33)$, respectively, so that

TABLE I. Ξ-meson coupling constants. The "quark model" values 1/3 for $g_{\sigma\Xi}/g_{\sigma N}$ in the first row and for $g_{\omega\Xi}/g_{\omega N}$ in the second row come from the naive quark counting, and −0.4 for $f_{\omega\Xi}/g_{\omega\Xi}$ from a quark model in Ref. [16].

Coupling	Fitted (a)	Fitted (b)	Quark model
$g_{\sigma\Xi}/g_{\sigma N}$	0.497	0.497	1/3
$g_{\omega\Xi}/g_{\omega N}$	0.5733	0.5663	1/3
$f_{\omega\Xi}/g_{\omega\Xi}$	−0.8	−0.8	−0.4

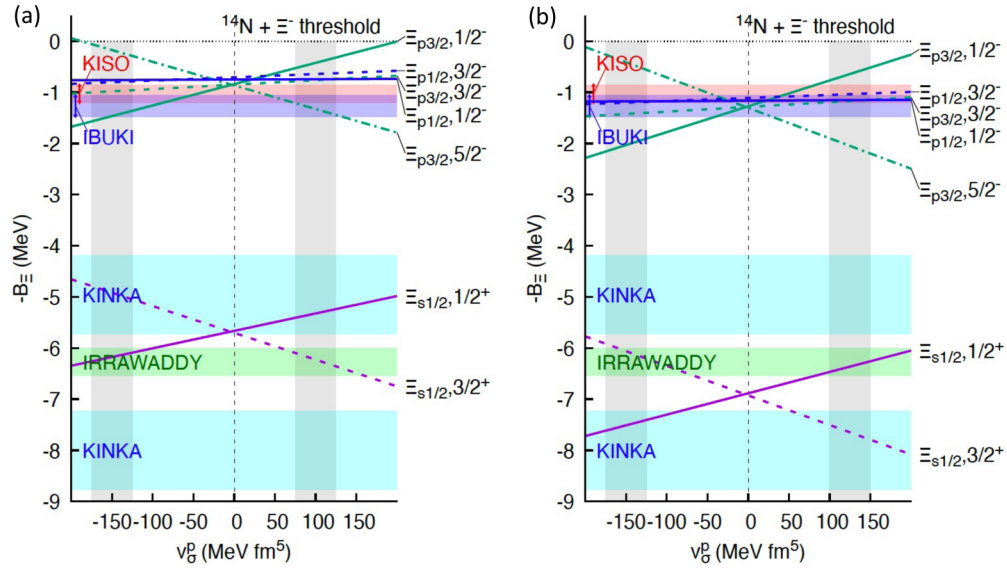

FIG. 1. The estimated energy spectrum of the $^{15}_{\Xi}$C nucleus as a function of the p-wave spin-spin interaction strength v_σ^p. Shown by lines are the energies of the levels labeled by the orbital occupied by the Ξ^- particle, Ξ_{lj}, and the total spin-parity, J^π. The experimental data of B_{Ξ^-} are shown by colored bands. The measured binding energy of KISO event was reported in Refs. [6,7], IRRAWADDY and KINKA events in Ref. [10], and IBUKI event in Ref. [9]. For KISO and KINKA events there are two possibilities each that correspond to the ground and an excited state of the decay products. For the parameter set (a) in Table I, we regard KINKA event at $E_\Xi = -4.96$ MeV as the ground state for the fit, while KINKA event at $B_{\Xi^-} = -8$ MeV is adopted for the fit in the parameter set (b).

$V_\beta^{\rm HAL}(R_\beta) = 0$. As a result, the factors $f_\beta(r)$ suppress the repulsive cores of the HAL potential, which would induce the short-range correlation missing in our simple framework. Also, we take zero-range reduction of the RMF meson-exchange interaction for the set (a) (set (b)) in Table I [19,20]:

$$\alpha = -\frac{g_{\sigma N} g_{\sigma \Xi}}{m_\sigma^2} + \frac{g_{\omega N} g_{\omega \Xi}}{m_\omega^2} = -327\ (-342)\ \text{MeV fm}^3. \quad (25)$$

Thus, finally, we employ

$$v_\sigma = (V_\sigma/V_0)\alpha = 4.87\ (5.09)\ \text{MeV fm}^3, \quad (26)$$

$$v_\tau = (V_\tau/V_0)\alpha = 26.83\ (28.05)\ \text{MeV fm}^3, \quad (27)$$

$$v_{\sigma\tau} = (V_{\sigma\tau}/V_0)\alpha = -53.56\ (-55.98)\ \text{MeV fm}^3, \quad (28)$$

where $V_0 = -201$ MeV fm^3 for the selection $t/a = 12$ in the lattice QCD calculation. Among the spin and isospin dependent terms of the ΞN interaction given in Eq. (22), only v_σ contributes to the binding energy of $^{15}_{\Xi}$C since the core is the isospin $T = 0$ nucleus, ^{14}N. As seen in Eq. (26), the value v_σ is rather small so that we cannot reproduce the spin-doublet state of IRRAWADDY and KINKA events by the s-wave interaction. It should also be noted that the HAL potential provides the s-wave ΞN interaction only, and a missing part of the ΞN interaction, p-wave spin and isospin dependent terms, might be important in $^{15}_{\Xi}$C since the core ^{14}N is a p-shell nucleus.

Next, we introduce a p-wave spin dependent interaction defined by

$$V_{N\Xi}^p = \sum_{i \in \text{nucleons}} v_\sigma^p \boldsymbol{\Sigma}_i \cdot \boldsymbol{\Sigma}_\Xi \overleftarrow{\nabla} \cdot \delta(\boldsymbol{r}_i - \boldsymbol{r}_\Xi) \overrightarrow{\nabla}, \quad (29)$$

where v_σ^p is parameter to be optimized by IRRAWADDY and KINKA events. In this work, we do not include $\Lambda\Lambda$-ΞN coupling for the following reason: The $\Lambda\Lambda$-ΞN coupling of the HAL potential is very small. For instance, in Ref. [21], the $NNN\Xi$ four-body system was predicted to have a bound state with very small decay width (0.05 MeV) related to $\Lambda\Lambda$-ΞN coupling. From this fact, it is expected that the decay width is small in the present work.

First, assuming IRRAWADDY is the ground state of $^{15}_{\Xi}$C, Fig. 1(a) shows the energy spectrum of $^{15}_{\Xi}$C as a function of p-wave spin-spin interaction v_σ^p. We see that, for the negative value of $v_\sigma^p \approx -150$ MeV fm^5, the energies of $J = 1/2^+$ and $3/2^+$ are in good agreement with IRRAWADDY event and KINKA events, respectively. In this case, IRRAWADDY event (KINKA event) can be interpreted as an observation of the ground (excited) state. On the other hand, for the positive value of $v_\sigma^p \approx 100$ MeV fm^5 the energies of $J = 3/2^+$ and $1/2^+$ are in good agreement with IRRAWADDY event and KINKA events, respectively. In this case, IRRAWADDY event (KINKA event) can be interpreted as an observation of the ground (excited) state, too. Next, assuming the lower part of KINKA event is the ground state of $^{15}_{\Xi}$C, for the negative value of $v_\sigma^p \approx -150$ MeV fm^5, KINKA event (IRRAWADDY event) can be interpreted as the observation of the $J^\pi = 1/2^+$ ($J^\pi = 3/2^+$) state, while for the positive value of $v_\sigma^p \approx 125$ MeV fm^5, KINKA event (IRRAWADDY event) can be interpreted as the observation of the $J^\pi = 3/2^+$ ($J^\pi = 1/2^+$) state.

It should be noticed that the optimized p-wave ΞN interaction is more or less the same magnitude as the p-wave N-Ξ NLO interaction in chiral effective field theory in Ref. [2].

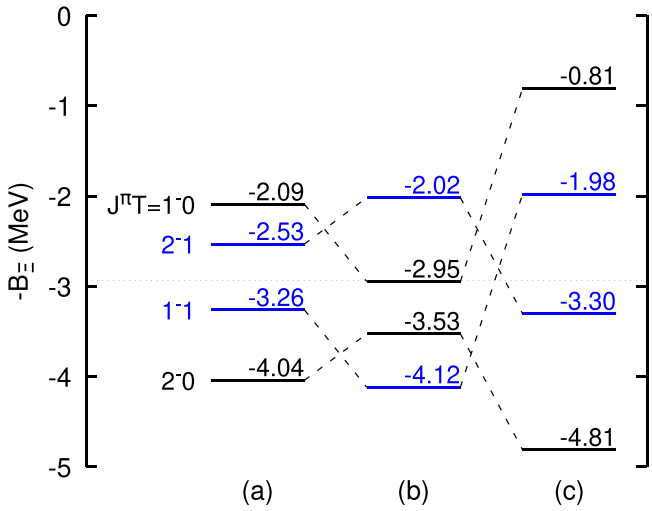

FIG. 2. The estimated energy spectra of the $^{12}_{\Xi}$Be nucleus, in which Ξ^- occupies the $1s$ state. (a) shows the spectrum calculated by RMF with the s-wave interaction as given in Eq. (22). The parameter set (a) in Table I is adopted. (b) and (c) represent the spectra calculated by RMF with the p-wave interaction as given in Eq. (29) together with the s-wave interaction. The spectrum (b) is obtained with a repulsive p-wave interaction $v_\sigma^p = 100$ MeV fm^5, while the spectrum (c) is with an attractive p-wave one $v_\sigma^p = -150$ MeV fm^5. The four states obtained with RMF without the residual interactions are degenerate and the energy is shown by the straight dotted line. The energies of the levels are shown in units of MeV.

B. Energy spectra of $^{12}_{\Xi}$Be

Figure 2 shows the estimated energy spectra of the $^{12}_{\Xi}$Be nucleus, in which Ξ^- occupies the $1s$ state. The parameter set (a) in Table I is adopted in the following calculations. Figure 2(a) shows the spectrum calculated by RMF with only the s-wave interaction as given in Eq. (22). Figures 2(b) and 2(c) represent the spectra calculated with the p-wave interaction as given in Eq. (29) as well as the s-wave interaction. The spectrum (b) is obtained with a repulsive p-wave interaction $v_\sigma^p = 100$ MeV fm^5, while the spectrum (c) is with an attractive one, $v_\sigma^p = -150$ MeV fm^5. The four states by RMF results without the residual interactions are degenerate and the energy is shown by the straight dotted line.

In Fig. 2(a), we illustrate the spectra calculated with the HAL potential. We see that the ground state of $^{12}_{\Xi}$Be becomes $T = 0, J^\pi = 2^-$. Qualitatively, the spectrum in Fig. 2(a) with the s-wave interaction can be understood in the following argument. Since the $\sigma\tau$ term is dominant in the s-wave interaction, we demonstrate the s-wave effect to calculate the two-body $N\Xi$ matrix element, taking only the spin-isospin operators,

$$\Delta E \propto \left\langle \left[N1p_{3/2}^{-1}\ \Xi nl_j \right]^{J^\pi T} \middle| \boldsymbol{\sigma}_N \cdot \boldsymbol{\sigma}_\Xi \vec{\tau}_N \cdot \vec{\tau}_\Xi \middle| \left[N1p_{3/2}^{-1}\ \Xi nl_j \right]^{J^\pi T} \right\rangle. \tag{30}$$

The isospin part is estimated to be

$$\langle T | \vec{\tau}_N \cdot \vec{\tau}_\Xi | T \rangle = \begin{cases} 1 & \text{for } T = 1, \\ -3 & \text{for } T = 0. \end{cases} \tag{31}$$

The spin part of Eq. (30) is also calculated as the reduced matrix form

$$\begin{aligned} &\left\langle \left[\nu 1p_{3/2}^{-1}\ \Xi nl\, j \right]^{J^\pi T} \middle\| \boldsymbol{\sigma}_N \cdot \boldsymbol{\sigma}_\Xi \middle\| \left[\nu 1p_{3/2}^{-1}\ \Xi nl\, j \right]^{J^\pi T} \right\rangle \\ &= (-)^{(J+1)} \begin{Bmatrix} 1/2 & 3/2 & J \\ 3/2 & 1/2 & 1 \end{Bmatrix} \\ &\quad \times \langle p_{3/2} \| \boldsymbol{\sigma} \| p_{3/2} \rangle \langle s_{1/2} \| \boldsymbol{\sigma}_\Xi \| s_{1/2} \rangle, \end{aligned} \tag{32}$$

where we use the $6j$ symbol, which is given by

$$(-)^{(J+1)} \begin{Bmatrix} 1/2 & 3/2 & J \\ 3/2 & 1/2 & 1 \end{Bmatrix} = \begin{cases} -\left(\frac{1}{40}\right)^{1/2} & \text{for } J = 2, \\ +\left(\frac{5}{24}\right)^{1/2} & \text{for } J = 1. \end{cases} \tag{33}$$

For the spin-isospin channel, the strength $v_{\sigma\tau}$ is attractive so that the $J = 2$, $T = 0$ state obtains the most attractive energy, while $J = 1$, $T = 0$ receives the most repulsive effect in Fig. 2(a). For the $T = 1$ state, the spin-isospin interaction works in opposite directions because of Eq. (31), which makes smaller contributions for $J = 2$, $T = 1$ and $J = 1$, $T = 1$ states,, compared with $T = 0$ states. Mathematical structures of p-wave interactions are more complicated, but essentially follow the features of s-wave interactions for the attractive p wave in Fig. 2(c), where both the s- and p-wave interactions work coherently. For the repulsive p-wave case in Fig. 2(b), two interactions cancel partially for $T = 0$ states, but the net effect gives more energy shift for $T = 1$ states than $T = 0$ states.

For the parameter set (b) in Table I, the energy spectra in Fig. 2 are essentially the same, but shifted downward by about 1 MeV as a whole.

C. Ξ mean field potential and Ξ single-particle energy

With the parameters thus obtained, we discuss the isoscalar part of the Ξ mean field potential,

$$V_{\sigma+\omega} = g_{\sigma\Xi}\sigma + g_{\omega\Xi}\omega^0, \tag{34}$$

for various single-Ξ hypernuclei with mass $A = 12$ to 209 shown in Fig. 3. The potential increases smoothly from the center to the surface without a plateau in the interior part of Ξ potential for the mass $A \leqslant 20$. The central depth is -20 MeV for the ^{11}B core and gradually become shallower for ^{14}N and ^{16}O cores. For heavier Ξ hypernuclei with $A \geqslant 40$, the central part of the potential becomes flat and the depth converges to around -12 MeV in heavier systems, which can be considered as an infinite matter limit. The width of the potential increases to follow an $A^{1/3}$ law. For the parameter set (b) in Table I, the potential depth for heavier nuclei becomes 2 MeV deeper than that of parameter set (a).

The single-particle states of Ξ hypernuclei with mass $A =$ 12 to 209 are shown in Fig. 4: (a) for Ξ^- with the Coulomb interaction between a Ξ^- particle and core protons; (b) for Ξ^0 without the Coulomb interaction. The Coulomb interaction between Ξ^- and protons is attractive and makes the potential depth deeper, about -17 MeV for the ^{208}Pb core and -2 MeV in the ^{11}B core. In Fig. 4(a), a Ξ particle in s orbit of $^{209}_{\Xi}$Tl is bound by 27 MeV, while that in the light nucleus $^{12}_{\Xi}$Be is bound by 3 MeV. In $^{209}_{\Xi}$Tl, the orbits only up to $l = 8$ are shown although there are a lot more Coulomb-assisted bound states. Only the s orbit is bound in the Ξ mean field potential

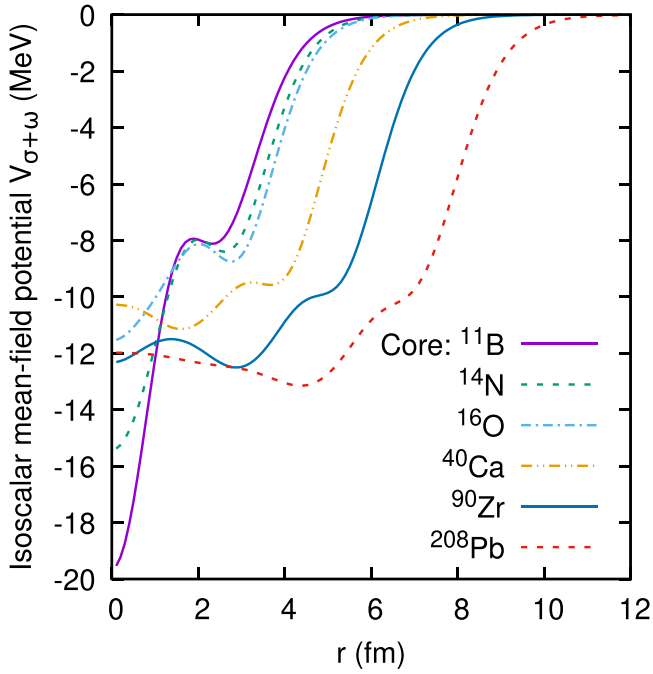

FIG. 3. The isoscalar part $V_{\sigma+\omega}$ of the mean field potential for the Ξ particle in light to heavy hypernuclei with $A = 11$–208 cores. The parameter set (a) is adopted in RMF calculations.

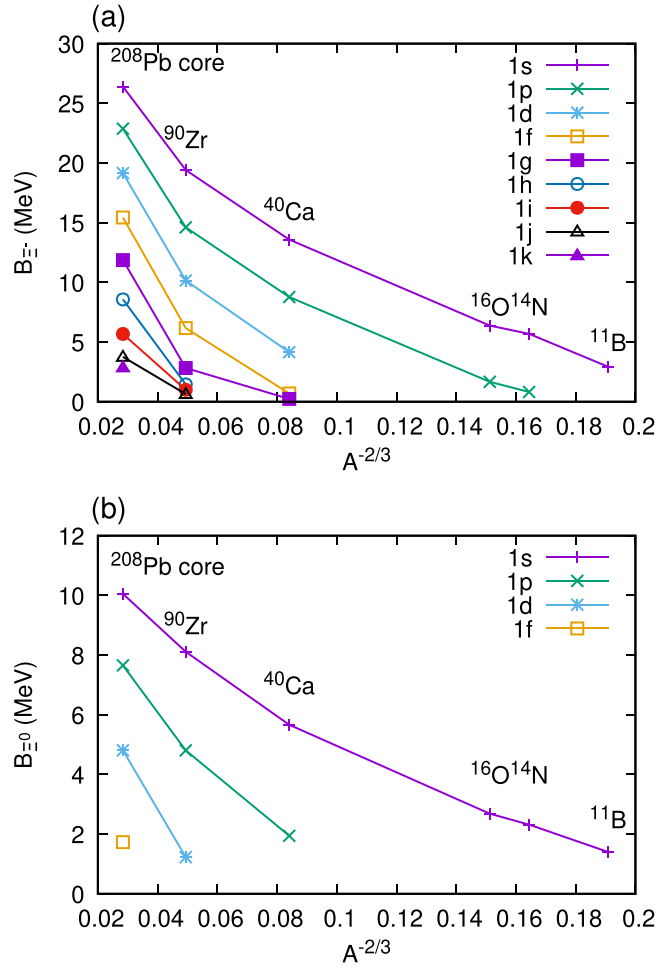

FIG. 4. Binding energies of single Ξ states: (a) for the Ξ^- particle and (b) for the Ξ^0 particle in light to heavy hypernuclei with a mass $A = 11$–208 core. The difference between (a) and (b) is with and without Coulomb interaction between Ξ particle and protons. The parameter set (a) is adopted in RMF calculations.

of $^{12}_{\Xi}$Be. Due to the contribution of the Coulomb interaction, the behavior of the single-particle energies of Ξ^- hypernuclei is similar to that of Λ hypernuclei [19].

In Fig. 4(b), the s-orbit is bound in all Ξ^0 nuclei starting from the ^{11}B core to the ^{208}Pb core. The binding energy of the s orbit of the ^{208}Pb core is about 10 MeV, which is almost the same as the potential depth. For $A = 11$, 14, and 16 cores, only the s orbit is bound, but the p orbit of the Ξ^0 hypernucleus becomes bound for the $A \geqslant 40$ core. For the ^{208}Pb core, the states with the angular momentum $l \leqslant 3$ are bound.

IV. SUMMARY

We studied the energy spectra of Ξ hypernuclei $^{15}_{\Xi}$C and $^{12}_{\Xi}$Be with an RMF model taking into account meson exchange $N\Xi$ interactions. The mean field potential parameters are optimized to reproduce the average energy of KINKA and IRRAWADDY events for possible ground states and also the average energy of KISO and IBUKI events for possible excited states in $^{15}_{\Xi}$C. We further introduce the two-body s-wave interaction between valence nucleons and the Ξ particle. The strength of the s-wave interaction is extracted from HAL lattice QCD calculations, which gives a strong attraction in the $(T, S) = (0, 0)$ channel. We demonstrate that the HAL s-wave interaction has rather small effect on the energy of $^{15}_{\Xi}$C since the core nucleus ^{14}N has the isospin $T = 0$ and the isoscalar spin-spin interaction is rather small. We then introduced the p-wave $N\Xi$ interaction to fit the energy difference between IRRAWADDY and KINKA events, and found that both repulsive and attractive spin-spin p-wave $N\Xi$ interactions give a reasonable energy splitting with the coupling strength $v_\sigma^p = -$ or 100 MeV fm^5, respectively. The attractive p wave gives $J^\pi = 1/2^+, 3/2^+$ states for the ground state and the first excited state, respectively. On the other hand, the repulsive one gives a reversed spectrum, i.e., $J^\pi = 3/2^+, 1/2^+$ states for the ground state and the first excited state, respectively. These p-wave coupling strengths give also a reasonable energy for IBUKI event as an excited Ξp state.

The energy spectrum of $^{12}_{\Xi}$Be is also studied in the same theoretical model. The HAL s-wave interaction in the spin-isospin channel is strongly attractive so that the $(J^\pi, T) = (2^-, 0)$ state becomes the lowest ground state and the states with $(J^\pi, T) = (1^-, 1)$, $(2^-, 1)$, and $(1^-, 0)$ become the excited states in order. When the p-wave interaction is introduced, the attractive p-wave one gives more attractive energy for $(J^\pi, T) = (2^-, 0)$ state, while the repulsive interaction cancels largely with the s-wave contribution and makes $(J^\pi, T) = (1^-, 1)$ the ground state.

The mean field $N\Xi$ potential of the present RMF model gives the potential depth $-(12$–$14)$ MeV in the nuclear matter limit. This potential depth is one-fourth of the nuclear mean field and half of the $N\Lambda$ mean field.

ACKNOWLEDGMENTS

We would like to thank to Prof. Nakazawa for helpful discussion of the present work. This work was supported in part by JSPS KAKENHI, Grants No. JP19K03858, No. JP19K03861, and No. JP20H00155, Grand-In-Aid for scientific Research on Innovative Areas, 18H05407, and and the National Natural Science Foundation of China (Grant No. U2032141).

[1] M. M. Nagels, Th. A. Rijken, and Y. Yamamoto, Extended-soft-core baryon-baryon model ESC16. III. $S = -2$ hyperon-hyperon/nucleon interactions, Phys. Rev. C **102**, 054003 (2020).

[2] J. Haidenbauer, U.-G. Meißner, and S. Petschauer, Strangeness $S = -2$ baryon-baryon interaction at next-to-leading order in chiral effective field theory, Nucl. Phys. A **954**, 273 (2016); J. Haidenbauer and U.-G. Meißner, In-medium properties of a ΞN interaction derived from chiral effective field theory, Eur. Phys. J. A **55**, 23 (2019).

[3] H. Takahashi *et al.*, Observation of a ${}^{6}_{\Lambda\Lambda}$He Double Hypernucleus, Phys. Rev. Lett. **87**, 212502 (2001).

[4] A. Ichikawa, Ph.D. thesis, Kyoto University, 2001 (unpublished).

[5] H. Ekawa *et al.*, Observation of a Be double-Lambda hypernucleus in the J-PARC E07 experiment, Prog. Theor. Exp. Phys. **2019**, 021D02 (2019).

[6] K. Nakazawa *et al.*, The first evidence of a deeply bound state of $\Xi^- - {}^{14}$N system, Prog. Theor. Exp. Phys. **2015**, 33D02 (2015).

[7] E. Hiyama and K. Nakazawa, Structure of $S = -2$ hypernuclei and hyperon hyperon interactions, Annu. Rev. Nucl. Part. Sci. **68**, 131 (2018).

[8] T.-T. Sun, E. Hiyama, H. Sagawa, H.-J. Schulze, and J. Meng, Mean-field approaches for Ξ^- hypernuclei and current experimental data, Phys. Rev. C **94**, 064319 (2016).

[9] S. H. Hayakawa *et al.*, Observation of Coulomb-Assisted Nuclear Bound State of $\Xi^- - {}^{14}$N System, Phys. Rev. Lett. **126**, 062501 (2021).

[10] M. Yoshimoto *et al.*, First observation of a nuclear s-state of a Ξ hypernucleus, ${}^{15}_{\Xi}$C, Prog. Theor. Exp. Phys. **2021**, 073D02 (2021).

[11] J. Boguta and A. R. Bodmer, Relativistic calculation of nuclear matter and the nuclear surface, Nucl. Phys. A **292**, 413 (1977).

[12] W.-H. Long, J. Meng, N. Van Giai, and S.-G. Zhou, New effective interactions in relativistic mean field theory with nonlinear terms and density-dependent meson-nucleon coupling, Phys. Rev. C **69**, 034319 (2004).

[13] J. Mareš and B. K. Jennings, Relativistic description of Λ, Σ, and Ξ hypernuclei, Phys. Rev. C **49**, 2472 (1994).

[14] Particle Data Group, Review of particle physics, Prog. Theor. Exp. Phys. **2020**, 083C01 (2020).

[15] J. Guo, X.-R. Zhou, and H.-J. Schulze, Skyrme force for all known Ξ^- hypernuclei, Phys. Rev. C **104**, L061307 (2021).

[16] J. Cohen and H. J. Weber, Relativistic σ-ω mean-field theory for hyperons from a quark model, Phys. Rev. C **44**, 1181 (1991).

[17] J.-N. Hu, Y. Zhang, and H. Shen, The Ξ-nuclear potential constrained by recent Ξ^- hypernuclei experiments, J. Phys. G: Nucl. Part. Phys. **49**, 025104 (2022).

[18] K. Sasaki *et al.*, ΛΛ and $N\Xi$ interactions from lattice QCD near the physical point, Nucl. Phys. A **998**, 121737 (2020).

[19] Y. Tanimura and K. Hagino, Description of single-Λ hypernuclei with a relativistic point-coupling model, Phys. Rev. C **85**, 014306 (2012).

[20] T. Bürvenich, D. G. Madland, J. A. Maruhn, and P.-G. Reinhard, Nuclear ground state observables and QCD scaling in a refined relativistic point coupling model, Phys. Rev. C **65**, 044308 (2002).

[21] E. Hiyama, K. Sasaki, T. Miyamoto, T. Doi, T. Hatsuda, Y. Yamamoto, and Th. A. Rijken, Possible Lightest 4Ξ Hypernucleus with Modern ΞN interaction, Phys. Rev. Lett. **124**, 092501 (2020).